Machine tool characterization and machining strategies for energy efficient manufacturing

Bert Lauwers[1], Yansong Guo [1]

[1]Department of Mechanical Engineering, KU Leuven, Leuven, Belgium

Abstract

This paper describes a brief overview of on-going activities performed on a Mori Seiki NL2000Y/500 mill-turn center, made available to the KU Leuven by the Machine Tools Technologies Research Foundation (MTTRF). Besides the extensive use of the equipment for educational activities, research is mainly focused on energy efficient manufacturing. Based on developed models for surface roughness and energy consumption of machine tools, an approach has been developed to optimize energy consumption in a "turning – grinding" sequence. In order to avoid the time consuming tuning of the above energy models (specific for each machine tool), a more generic bottom-up approach is being developed based on the energy consumptions of machine tool components, in this research applied on the Mori Seiki NL2000Y/500.

Keywords: Energy Consumption, Energy Efficient Machining Strategies, Machine Tool Characterization

1 INTRODUCTION

Currently, tremendous energy and resource consumption in manufacturing industry has become increasingly essential. As reported in [1], 14.3% of the European industrial electricity consumption is attributed to the metal processing industry, which results in substantial environmental issues. In addition, inevitable rising costs of energy resources also inspires manufacturing enterprises to implement green production. In this context a paradigm shift towards environmentally friendly manufacturing is evoked [2], and minimizing production energy has been acknowledged as one of the main objectives.

As machine tools are the key elements in production, reducing the embodied carbon footprint of products can effectively be achieved by reducing the energy consumption of machine tools. Diaz et al. [3] as well as Kara and Li [4] depicted that the energy consumption can be reduced by selecting higher material removal rates. Mativenga and Rajemi [5] proposed a method to optimize the cutting parameters with minimum energy based on optimum tool life. Furthermore, a surface roughness based approach was developed by Guo et al. [6] to optimize machining parameters in terms of energy minimization, the results were also presented at the MTTRF 2012 annual meeting [7].

Compared to turning, grinding possesses mostly requires higher specific energy, normally one order of magnitude higher [8]. Therefore it can be expected that minimizing the material volume of grinding will effectively reduce the total manufacturing energy. Therefore, in a "turning – grinding" sequence, applied for the precise machining of axi-symmetric parts, the more material is machined by turning, the less energy will be consumed.

This paper makes a comparison between turning and grinding (from energy point of view) and makes a proposal how the grinding stock can be optimized based on minimizing energy consumption. This proposed approach (described in section 3) is based on energy and surface models developed for specific machine tools (section 2). The used energy model is developed for a machine tool as a whole, meaning that the model should be tuned for each specific machine tool, requiring quite some calibration work. Therefore, a more generic approach has also been developed and applied, where main energy consuming machine tool components are energetically characterized Within this research, the spindle, the drives (X,Y,Z) and the turret (with driven tools) have been characterized for the Mori Seiki NL2000Y/500 (section 4.1,4.2,4.3). Knowing the energy consumption of machine tool components is also important for the development of machine tool models as it is being developed within the EU-project DEMAT (section 4.4).

2 ENERGY AND SURFACE MODELS FOR TURNING AND GRINDING

As described in last year's MTTRF paper [7], a two-step approach has been developed in order to select finishing parameters in terms of minimum specific energy. As illustrated in Figure 1, a roughness model is used to determine a process settings window, giving the required surface roughness. In a second step, process parameters that result in minimum energy can be selected by applying a specific energy model.

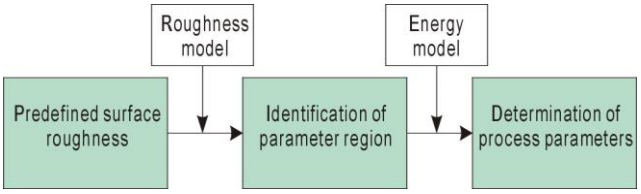

Figure 1: Procedure for optimal parameter selection [7].

In this research, also described in [6,7], an energy model was derived for the Mori Seiki NL2000Y/500 and given in equation (1).

$$TSE = C_0 \cdot v_c^{e_1} \cdot f^{e_2} \cdot a_p^{e_3} \cdot D^{e_4} + \frac{C_1}{v_c \cdot f \cdot a_p} \quad (1)$$

The Total Specific Energy (TSE, J/mm^3) is used to evaluate the energy consumption of machine tools. It is composed of the Specific Process Energy (SPE, J/mm^3) and the Specific Constant Energy (SCE, J/mm^3), which indicate respectively the variable and the constant power. The parameters are v_c (cutting speed, [m/min]), f (feed rate, [mm/rev]), a_p (cutting depth, [mm]) and D (final workpiece diameter, [mm]). The coefficients were derived for turning

steel “11SMnPb30” on the Mori Seiki NL2000Y/500: e_1: 0.4486; e_2: -0.6851; e_3: -0.8214;e_4:-0.8040; C_0: 1.9205; C_1: 85.4442.

In order to perform an optimization for parts, requiring turning and grinding, similar energy models (equation (2)) have been derived within this research for a grinding.

$$TSE = C_0^{'} \cdot v_w^{e_1^{'}} \cdot f^{e_2^{'}} \cdot a_p^{e_3^{'}} \cdot v_s^{e_4^{'}} D^{e_5^{'}} + \frac{C_1^{'}}{v_w \cdot f \cdot a_p} \quad (2)$$

with v_w the workpiece speed [m/min]; f the feed rate [mm/rev]; a_p the cutting depth [mm]; v_s the grinding wheel speed [m/s] and D the final workpiece diameter [mm]. To identify the constants and coefficients in equation (2), cylindrical traverse grinding experiments were carried out also in steel “11SMnPb30” on a grinding machine “Studer S20” (CBN grinding wheel, thickness: 10mm, v_w: 25 ~ 250 m/min; f: 0.225 ~ 2.25 mm/rev; a_p: 0.3 ~ 15 µm; v_s: 20, 25.5 m/s; coolant applied). Based on these experiments, the following parameters were derived for equation (2) (with a R-square coefficient of 0.999), e'_1: -0.8912; e'_2: -0.9750; e'_3: -0.9352; e'_4: 0.4117; e'_5: -0.0642; C'_0: 12.3237; and C'_1: 56.4964.

Based on both energy models, the feed, the cutting depth and the cutting speed present a large influence on the energy consumption. The constant C_1 reflects the constant power demand of the machine; and compared to the measured constant power 1320 W for the investigated turning machine, the modeled value is 1424 W. For the grinding machine, the measured constant power is 957.2 W, while he modeled power is 941.6W.

Roughness models used in this research for turning [9] and grinding [10] are presented in the equations (3) and (4).

$$R_{z\_turning} = C \cdot v_c^n \cdot f^p \cdot a_p^m \quad (3)$$

$$R_{z\_grinding} = C^{'} \cdot \left(\frac{v_w}{v_s}\right)^{\alpha} \cdot \left(\frac{a_p \cdot f}{b_s / 2}\right)^{\beta} \quad (4)$$

Table 1 lists the fitted constants for the equations (3) and (4) for turning and grinding, obtained through experiments performed within this research. It can be noticed that the surface roughness in both processes can be improved by applying lower feed and lower cutting depths. In turning, higher cutting speed results in better surface roughness. In grinding, the surface quality can be enhanced through higher speed ratios (v_s/v_w) [11].

Table 1: Fitted constants for surface roughness model

Turning	C=102.5518; n=-0.2676
(R^2=0.9)	p=0.595; m=0.0552
Grinding	C’=8.9501; α= 0.0527
(R^2=0.85)	β= 0.1165

3 MACHINING STRATEGIES FOR AXI-SYMMETRIC PARTS

Grinding is often applied as a finishing process for parts where high precision is required. Grinding however owns lower material removal rate and requires higher specific energy [8], but it also presents several advantages in dimension and shape accuracy and surface quality. Therefore, comparison of both processes needs to be carried out for each specific application, but energy evaluation could also be taken into account.

3.1 Comparison of turning and grinding

Turning and grinding are comparable in a region where the same product requirements (in this research, the surface roughness) can be satisfied. With the parameter limits of the cutting tools and machines, the surface roughness boundaries can be determined by using the equations (3) and (4). For finish turning, the parameter settings used for the Mori Seiki NL2000Y/500 are recommended by the tool suppliers [12] (vc:190 ~ 250 mm/min; f: 0.05 ~ 0.15 mm/rev; a_p: 0.5 ~ 2 mm). The grinding parameters are constrained by the investigated machine Studer S20 (v_w: 25 ~ 250mm/min; f: 0.225 ~ 2.25 mm/rev; a_p 0.3 ~ 15 µm; v_s: 20; 25.5 m/s. As a result of these experiments, the lower roughness limit ($R_{z,GL}$) and upper roughness limit ($R_{z,GU}$) of grinding are 2.38µm and 5.64µm.The lower turning limit ($R_{z,TL}$) is 3.80 µm. It is not necessary to calculate the upper turning limit since turning is the most basic cylindrical machining process. The overlap of the surface roughness for turning and grinding is from 3.80 µm to 5.64µm. Figure 2 shows schematically these intervals.

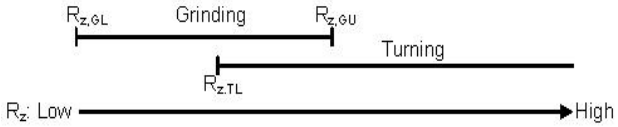

Figure 2: Surface roughness limits for turning and grinding.

To comply with a specified surface roughness, quantities of parameter combinations can be derived from the roughness model, and these diverse parameters would further lead to various specific energies. In order to constitute the “energy-surface roughness” relation, the minimum specific energy (TSE_{min}) can be used and the “TSE_{min} – Rz” relation refers to the minimum specific energy required for conforming to the specified roughness.

Figure 3 illustrates the comparison of “TSE_{min} - Rz” relation for turning and grinding. The minimum required specific energy increases while the surface roughness is enhanced. This shows that in finishing higher energy is required to acquire the final quality. Compared to turning, grinding presents a much steeper decline trend on the “TSE_{min} – Rz” relation. Moreover, the energy intensity of grinding is higher than finish turning over the compared region. Therefore in this case, if the required surface roughness is situated in the common surface roughness region (3.80µm ~ 5.64µm), turning can be chosen as the finishing process.

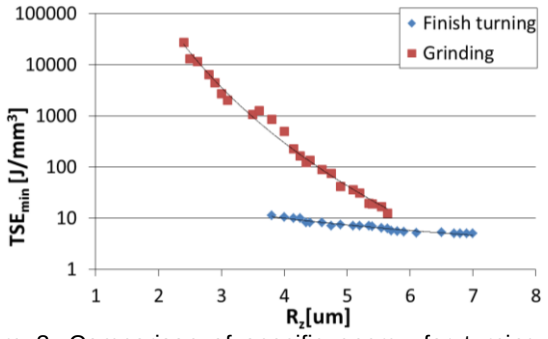

Figure 3: Comparison of specific energy for turning and grinding processes.

3.2 Machining boundary for turning-grinding

The stock allocation in process planning can affect remarkably the final manufacturing quality and the cost [13], hence it is very crucial to identify quantitatively the stock of every process for a specified production sequence.

Figure 2 presents the three essential surface roughness limits for turning and grinding – $R_{z,TL}$, $R_{z,GL}$ and $R_{z,GU}$. As turning is most energy efficient, the lower roughness limit of turning ($R_{z,TL}$) can be applied as the process switching point while optimizing the machining boundary of turning-grinding.

As grinding is an energy consuming process, the parameter setting of each grinding layer should be optimized in terms of minimizing the energy and satisfying the surface roughness assigned to every layer. Accordingly the most essential step is to establish the intermediate surface roughness "$R_{z(i)}$" of the grinding process which can be further applied to calculate for each ground layer its corresponding parameter "$v_{w(i)}$, $f_{(i)}$, $a_{p(i)}$, $v_{s(i)}$" in terms of minimum energy. As shown in Figure 4 the machining boundary between turning and grinding can be determined by stacking up the grinding depth "$a_{p(i)}$" of all constituted ground layers from the base line. The final development of this optimization procedure is now on-going at the KU Leuven.

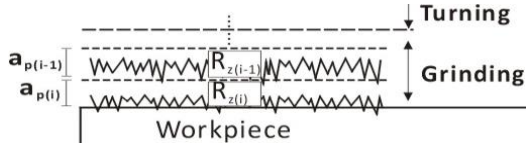

Figure 4: Machining boundary for turning-grinding.

4 MACHINE TOOL CHARACTERISATION

The above strategies are based on energy models which are derived for the machine tool as a whole. This means that the models (equations (1) and (2)) should be tuned for every specific machine tool. A more generic approach is presented in Figure 5, where the total power consumption is calculated based on a summation of different power consuming elements: material removal power (P_{mr}), axes movements P_{vt}, spindle rotation P_{vs}, driven tools on the turret P_{vdt} and the constant power P_c.

The material removal power (P_{mr}) is the effective power consumed in the cutting process and can be calculated based on the Victor-Kienzle formula. The constant power consumption (P_c) is not affected by the cutting parameters and is assigned to the pumps, controllers, fans, lighting and so on.

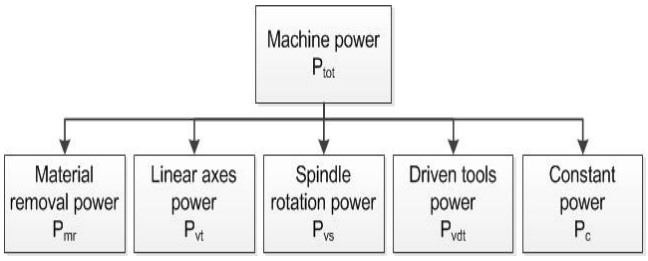

Figure 5: Decomposition of machine power.

When knowing the energy behavior of the different components of the machine tool (spindle, drives,..) it should be easier to calculate the consumed energy for various operations. These energy models (on component level) could be integrated into CAD/CAM systems for the calculation of energy consumption of machining operations.

Within this research, the spindle, drives and the turret of the Mori Seiki NL2000Y/500 has been energetically characterized, by performing around 245 experiments. During the experiments, it was noticed that the machine controllers already consume a constant power P_{vc} (in addition to the other constant power P_c) of 202,8 W (standard deviation: 14,7 W), which is due to the activation of the drives when the doors are closed.

4.1 Characterization of the spindle

The energy required to drive the spindle is a significant portion of the variable energy. Generally, the power consumption of the spindle can be written as:

$$P_{vs} = \frac{1}{\eta} \cdot ((I_{work\,piece} + I_{drive\,train}) \cdot \alpha \cdot \omega) + \frac{1}{\eta} \cdot P_w + P_{vc} \quad (5)$$

With $I_{workpiece}$ + $I_{drive\ train}$ the inertia of the spindle, α the acceleration, ω the speed, P_w the friction power (when there is no acceleration), P_{vc} (see above) and η the efficiency of the motor. In order to have the energy consumption over a certain time, the above formulae should be integrated. The acceleration α can also be negative (deceleration), which results for the Mori Seiki NL2000Y/500 in a negative power/energy, given back to the net.

4.1.1 Acceleration profile

The acceleration/deceleration profile, the inertia of the drive train, the friction power and the efficiency has been determined experimentally. For this purpose, experiments have been set up where the spindle was accelerated to different rotational speeds, which in turn were kept constant for 10 seconds (for the Mori Seiki NL2000Y/500, 21 experiments were set in the range of 50 to 5000 rpm).

The evolution of the rotation was measured based on pulse measurements (equation 6) of a reflective strip mounted on the chuck (Figure 6). Δt [s] is the time between two pulses.

$$\omega(t) = 2 \cdot \pi \cdot \frac{1}{\Delta t} \quad (6)$$

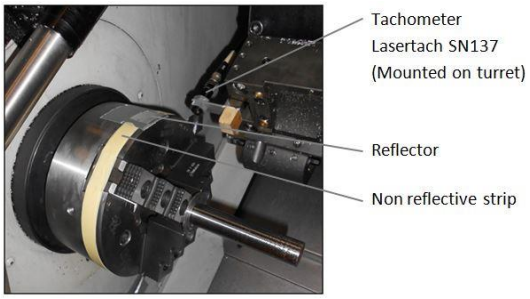

Figure 6: Arrangement of rotational speed measurements.

The evolution of the rotational speed as a function of time has been established for each of the 21 experiments. Moreover these experiments were executed for different configurations to examine the influence of the inertia of the workpiece on the acceleration profile. Each of the following configurations was subjected to the 21 experiments:

without workpiece in the chuck; with workpiece (I: 125kg.mm^2) in the chuck; with workpiece (I: 4568kg.mm^2) in the chuck. Figure 7 shows the results of the experiments without workpiece in the chuck.

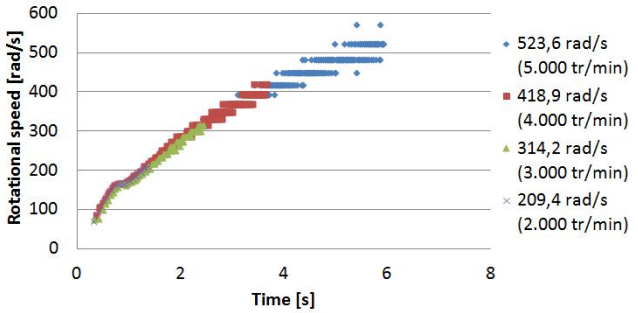

Figure 7: Rotation of the spindle as a function of time for the acceleration to different rotational values without workpiece in the chuck.

From Figure 7 it can be concluded that the rotation profile is independent of the rotation to which the spindle is accelerated. The course is also becoming 'wider' (horizontal clustering of data points) at higher rotations, which is due to the discrete nature of the determination of angular velocities with the tachometer. The evolution of the rotation $\omega(t)$ [rad/s] and the acceleration ($\alpha(t) = d\omega/dt$) is listed in Table 2.

Table 2: Velocity and acceleration profile of the spindle.

Time range	ω [rad/s]	α [rad/s^2]
0≤t<0.705	$\omega(t) = 234.3 * t$	α=234.3
0.705≤t≤0.895	ω = 165.3	α=0
t>0.895	$\omega(t) = 182{,}15 * t^{0.625}$	$\alpha(t)=113.8*t^{0.375}$

The course of the rotational values as a function of time can be divided into three parts. The first part is from 0 to 165,3 rad/s (linear relationship), a second part is keeping a constant rotation of 165,3 rad/s for some milliseconds and a third part is when the rotation is rising again (can be represented as a kind of power function).

Based on the results of all the experiments, executed on the different configurations, it could be concluded that the inertia has no significant influence on the rotation profile. The inertia of the drive train can be determined (equation (7)) if at certain times, when the spindle is accelerating, both power P_{vs_acc} and angular acceleration α_{acc} are known. The inertia of the drive train is 596.680 kg.mm² (standard deviation: 34.466 kg.mm²).

$$I_{drivetrain} = \frac{P_{vs\_acc} - P_w - P_h - P_{vc}}{\alpha \cdot \omega} - I_{workpiece} \qquad (7)$$

4.1.2 Friction power

In case of spindle turning at constant rotation, the variable spindle power consists only of the friction power. The friction power can be calculated using equation (8):

$$P_w = (P_{vs\_\omega cte} - P_{vc}) \cdot \eta \qquad (8)$$

with $P_{vs\_\omega cte}$ the measured power and P_{vc} as explained above. The evolution of the efficiency η of the spindle motor (Mitsubushi SJ-PMB25604-01') as a function of the rotation is not known, but has been estimated experimentally. Since the inertia of the drive train of the Mori Seiki NL2000Y/500 is constant during its whole rotational speed range (see further), the efficiency of the conversion from electrical to mechanical power has been derived for the efficiency of the drive train.

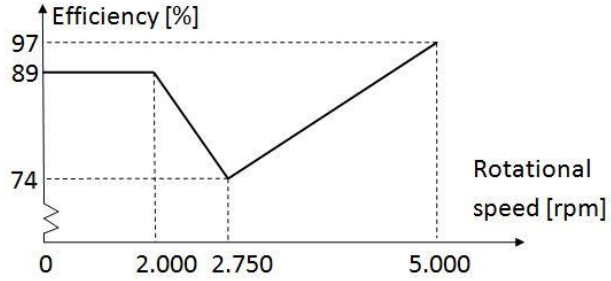

Figure 8: Efficiency as function of rotational speed of the spindle.

The friction power of the drive train as a function of the rotation has been determined by measuring the power at different constant rotations. In the series of experiments, prepared for the characterization of the spindle, the rotational speed for every experiment is kept constant for 10 seconds. The influence of the inertia of the workpiece has also been examined. The results of these experiments are shown in Figure 9. The curve corresponding to 0 kg.mm² sets the configuration for which no workpiece is clamped in the chuck. The inertia associated with the other curves represents the inertia of the workpiece clamped in the chuck. From this graph it shows that the inertia has no appreciable influence on the friction power. The division of the curve into 4 sub-curves (indicated by 1,2,3 and 4) is due to the fact that a new experimental program was started at these points. The beginning of these sub-curves is always slightly higher (compare to what the trend would suggest), but this variation is probably due to the cool down of the spindle oil at the end of each experimental program.

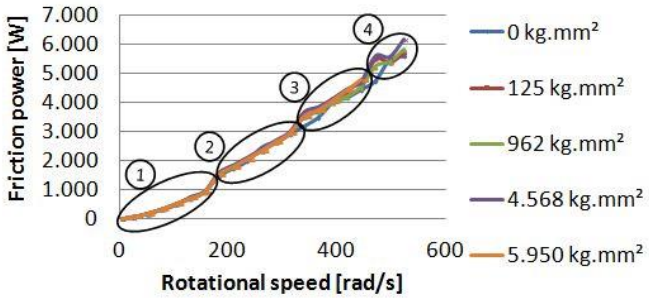

Figure 9: Friction power as function of angular velocity of the spindle for different inertias clamped into the chuck.

Based on the experimental data, the friction power Pw [W] as a function of ω [rad/s] can be described by equation (9).

$$P_w = 0.0102 \cdot \omega^2 + 6.0990 \cdot \omega \qquad (9)$$

This function has a strong linear and a rather light quadratic character. The strong linear character is a result of the prevailing coulomb friction. The quadratic character is due to the (small) viscous friction from the spindle and the oil around it.

4.2 Drives

The energy characterization of the three linear feed drives (X-, Y- and Z-drive) of the Mori Seiki NL2000Y/500 has been performed on a similar way as for the spindle. The feed axes have substantially smaller energy usage and certain feed rates can be reached in less than one second, making the acceleration energy usage negligible.

In Figure 10, Figure 11 and Figure 12 the energy consumption of the three drives is presented. For X- and Y-drive, the direction of movement has an important influence on the energy usage, since the gravitational force of the (heavy) turret.

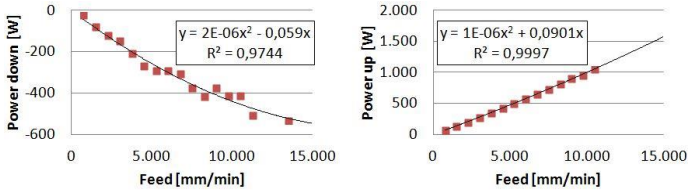

Figure 10: Power as function of feed for the X-drive – polynomial curve fit.

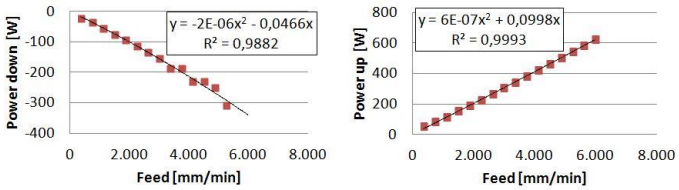

Figure 11: Power as function of feed for the Y-drive – polynomial curve fit.

For all the three graphs there is again a substantial linear and a small quadratic behavior. The linear behavior is again due to coulomb friction, as the quadratic behavior is due to viscous friction. Next equations for the power $P_{vtx/y/z}$ [W] model the power required to move a linear drive in certain direction with a certain feed $f_{x/y/z}$ [mm/min]:

$$
\begin{aligned}
P_{vtx} &= 0.000002 \cdot f_x^2 - 0.059 \cdot f_x \quad (\text{X - drive} \downarrow) \\
P_{vtx} &= 0{,}000001 \cdot f_x^2 + 0.0901 \cdot \text{fx} \quad (\text{X - drive} \uparrow) \\
P_{vty} &= -0{,}000002 \cdot f_y^2 - 0.0466 \cdot f_y \quad (\text{Y - drive} \downarrow) \\
P_{vty} &= 0.0000006 \cdot f_y^2 - 0.0998 \cdot f_y \quad (\text{Y - drive} \uparrow) \\
P_{vtz} &= 0.000000.8 \cdot f_z^2 - 0.0202 \cdot f_z \quad (\text{Z - drive})
\end{aligned}
\qquad (10)
$$

4.3 Turret with driven tools

In a similar way, the energy consumption of the drive (BMT® motor) within the turret (for driven tools) has been characterized and this for two configurations (tool rotating around X-axis or Z-axis). The inertia of the clamped tools is neglected compared to the inertia of the drive motor.

To measure the power, P_{vdt} and to derive a model for it, a series of experiments where the tool is rotating at a certain constant rotational speed for six seconds, were set up. By subtracting the constant part P_{vc} (in the power measurements) the variable energy consumption is given in Figure 13.

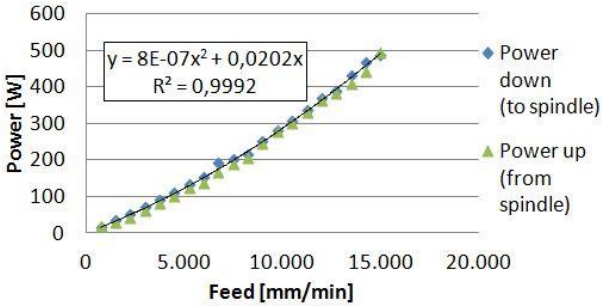

Figure 12: Power as function of feed for the Z-drive – polynomial curve fit.

It is clear that there is no difference in evolution for a tool which is rotating around the X-axis or the Z-axis. Therefore, all the data can be used to deduce one model (equation 11) that is applicable for both tool configurations.

$$P_{vdt} = 0.0007 \cdot \omega_{dt}^2 + 1.0323 \cdot \omega_{dt} \qquad (11)$$

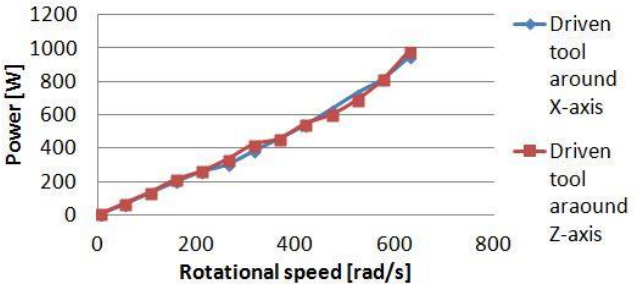

Figure 13: Power needed to rotate a certain tool configuration at a certain angular velocity.

4.4 Machine tool modeling: the DEMAT concept

Modelling of machine tool components is a research topic fitting within the EU FP7 project DEMAT (Dematerialised Manufacturing Systems: A new way to design, build, use and sell European Machine Tools). Within this project, KU Leuven is responsible for the concept development of machine tool models, which are used as a back bone for an Information Sharing Platform (ISP) or any other application (e.g. CAD/CAM)

The proposed modelling approach composes information of mechanical elements constituting hardware components of the machine tool (spindle, drives,…) and information about intangible entities such as kinematic links, market positioning, etc. The machine model is split into several sub-models, each dedicated to the different aspects, and, eventually, all of the sub-models are brought together by a UML diagram that represents various objects linked via different dependencies. Figure 14 shows an extract of a UML layout which can be applied on the Mori Seiki NL2000Y/500, showing also more detailed information about spindle and axes drives.

The UML diagrams developed within the DEMAT project also contain additional data describing the properties of the objects. These properties can be simple numerical fields, like mass, production costs, price, etc, or refer to more sophisticated descriptions, such as CAD geometry files, CAE model files, servomotor torque diagrams, controller

behaviour, and other data structures that can be seamlessly added because of the flexibility of the UML.

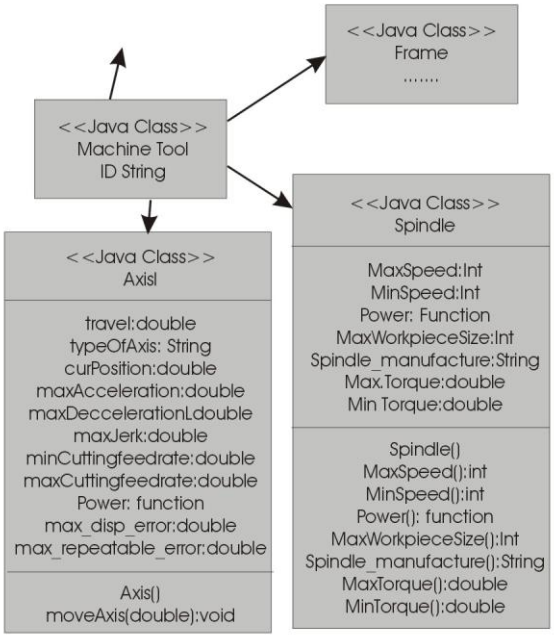

Figure 14: Extract of UML model for a machine tool structure with detailed information about the spindle and axes drives.

5 USE OF THE EQUIPMENT WITHIN EDUCATIONAL AND OTHER RESEARCH ACTIVITIES

The Mori Seiki NL2000Y/500 is extensively used in two bachelor courses ("Production Engineering and Systems (3rd year bachelor, mechanical engineering)"; "Machine Design and Construction (3rd year bachelor, agricultural engineering) and two master courses. In addition, the equipment has also been used in a master student project dealing with the machining of ZrO_2-based ceramics using ultrasonic vibration.

6 CONCLUSIONS

This paper briefly described two research activities performed on a turn-mill centre (Mori Seiki NL2000Y/500) made available by MTTRF to KU Leuven. Besides the extensive use of the machine within educational activities, research was focused on energy efficient machining strategies and machine tool characterization of energy consuming machine tool elements. It was shown that in a turning-grinding process sequence, it is better to machine as much as possible by grinding due to the higher specific energies in grinding. The different energy consuming components of the Mori Seiki NL2000Y/500 has been characterized, which forms the basis for the development of virtual machine tool models.

ACKNOWLEDGEMENT

The authors want to thank the Machine Tool Technologies Research Foundation (MTTRF) for the support in making a CNC Machining Center (Mori Seiki NL2000Y/500) available to the KU Leuven. In addition, the research has been made possible through the IWT project Eco2Cut (Institute for the Promotion of Innovation by Science and Technology in Flanders) and the EU project DEMAT (NMP2-SE-2010-246020). Also thanks to Ing. Dries Vandezande and Ing. Jochen Cobbaert, two master thesis students who very much supported the research on machine tool characterization.

REFERENCES

[1] European Commission, 2010, Energy –Yearly Statistics 2008, Eurostat Statistical Books, ISSN 1830-7833.

[2] Gutowski T., Murphy C., Allen D., Bauer D., Bras B., Piwonka T., Sheng P., Sutherland J., Thurston D., Wolff E., 2005, Environmentally benign manufacturing: Observations from Japan, Europe and the United States, Journal of Cleaner Production; Vol. 13/1, pp.1-17.

[3] Diaz N, Helu M, Jarvis A, Tönissen S, Dornfeld D., Schlosser R., 2009, Strategies for Minimum Energy Operation for Precision Machining. Proceedings of MTTRF 2009 annual meeting.

[4] Kara. S., Li W., 2011, Unit process energy consumption models for material removal processes, CIRP Annals – Manufacturing Technology, Vol.61/1, pp.37-40.

[5] Mativenga P.T., Rajemi M.F., 2011, Calculation of optimum cutting parameters based on minimum energy footprint. CIRP Annals – Manufacturing Technology; Vol.60/1, pp.149 – 152.

[6] Guo Y., Loenders J., Duflou J., Lauwers B., 2012, Optimization of energy consumption and surface quality in finish turning, Proceedings of 5th CIRP International Conference on High Performance Cutting, pp.512 – 517.

[7] Lauwers B., Ferraris E., Guo Y., Turning Research at KU Leuven using a Mori Seiki NL2000/Y500: Machinability Investigation of ZrO2 and Development of Models for Energy Efficient Machining , MTTRF 2012 Annual Meeting, Iga, Japan, 24-26 June 2012 (pp. 145-162).

[8] Ren Y.H., Zhang B., Zhou Z.X., 2009, Specific energy in grinding of tungsten carbides of various grain sizes, CIRP Annals – Manufacturing Technology, Vol.58/1, pp.299 – 302.

[9] Fang XD, Safi-Jahanshaki H., 1997, A new algorithm for developing a reference model for predicting surface roughness in finish turning of steels. International Journal of Production Research, Vol.35/1, pp. 179 – 197.

[10] Tönshof H.K., Peters J., Inasaki I., Paul T., 1992, Modeling and simulation of grinding processes, CIRP Annals – Manufacturing Technology, Vol.41/2.

[11] Hecker R.L., Liang S.Y., 2003, Predictive modeling of surface roughness in grinding, International Journal of Machine tools and Manufacture, Vol.43, pp.755-761.

[12] WNT Deutschland GmbH. Cutting condition for fine machining. Turning tool catalogue; 2011, pp.210.

[13] Tang G.R., Kung R., Chen J.Y., 1994, Optimal allocation of process tolerance and stock removals, Internation journal of production research, Vol. 32/1, pp.23 – 35.